Development 134, 1789-1797 (2007) doi:10.1242/dev.02837

Multiple functions of Snail family genes during palate development in mice

Stephen A. Murray, Kathleen F. Oram and Thomas Gridley*

Palate development requires precise regulation of gene expression changes, morphogenetic movements and alterations in cell physiology. Defects in any of these processes can result in cleft palate, a common human birth defect. The Snail gene family encodes transcriptional repressors that play essential roles in the growth and patterning of vertebrate embryos. Here we report the functions of Snail (*Snai1*) and Slug (*Snai2*) genes during palate development in mice. *Snai2*$^{-/-}$ mice exhibit cleft palate, which is completely penetrant on a *Snai1* heterozygous genetic background. Cleft palate in *Snai1*$^{+/-}$ *Snai2*$^{-/-}$ embryos is due to a failure of the elevated palatal shelves to fuse. Furthermore, while tissue-specific deletion of the *Snai1* gene in neural crest cells does not cause any obvious defects, neural-crest-specific *Snai1* deletion on a *Snai2*$^{-/-}$ genetic background results in multiple craniofacial defects, including a cleft palate phenotype distinct from that observed in *Snai1*$^{+/-}$ *Snai2*$^{-/-}$ embryos. In embryos with neural-crest-specific *Snai1* deletion on a *Snai2*$^{-/-}$ background, palatal clefting results from a failure of Meckel's cartilage to extend the mandible and thereby allow the palatal shelves to elevate, defects similar to those seen in the Pierre Robin Sequence in humans.

KEY WORDS: Cleft palate, Snail, Slug, Epithelial-mesenchymal transition, Periderm cells, Mouse

INTRODUCTION

Cleft palate, with or without cleft lip, represents one of the most common birth defects observed in humans, occurring in approximately 1 in 700 live births (Gorlin et al., 2001; Murray, 2002). Formation of the mammalian secondary palate begins with the appearance of bilateral outgrowths from the maxillary processes, which grow and extend vertically along the sides of the tongue (Ferguson, 1988). At a specific point in development, mechanical forces resulting from the forward extension of the mandible depress the tongue, allowing the palatal shelves to elevate and come into close approximation with each other. Through the specific expression of cell surface molecules and alterations in the morphology of cells along the medial edge epithelia (MEE), the shelves adhere and form a single structure bisected by a layer of epithelium, known as the medial epithelial seam (MES). The MES subsequently disappears, leading to a continuous palatal shelf consisting of a mesenchymal core bounded by the nasal and oral epithelium.

Disruption of any of these processes can result in cleft secondary palate. For example, *Tgfb3*-null mice exhibit defects in palatal shelf fusion resulting from a failure of the MEE to acquire the necessary adhesive phenotype (Gato et al., 2002; Taya et al., 1999; Tudela et al., 2002). Mutation of the *Msx1* gene, however, results in cleft palate due to reduced proliferation in the palatal shelves during the vertical growth phase (Zhang et al., 2002). Cleft palate is also seen in mice exhibiting defects in palatal shelf elevation, such as *Jag2*-null mice, in which fusions between the tongue and palatal shelves are observed (Casey et al., 2006; Jiang et al., 1998a).

The Pierre Robin Sequence (also termed Robin Sequence) is a human developmental malformation characterized by mandibular retrognathia (normal size receded mandible) or micrognathia (abnormally small mandible), glossoptosis (rearward and downward displacement of the tongue) and cleft palate. Cases of Pierre Robin Sequence are both phenotypically and genetically heterogeneous (Cohen, 1999; Houdayer et al., 2001; Jakobsen et al., 2006; Jamshidi et al., 2004; Melkoniemi et al., 2003; Ounap et al., 2005; Ricks et al., 2002). The association of mandibular defects with palatal clefting has been observed in several mouse models of cleft palate, including *Hoxa2* (Gendron-Maguire et al., 1993), *Egfr* (Miettinen et al., 1999) and *Dmm* (disproportionate micromelia, a dominant mutant allele of the *Col2a1* gene) (Ricks et al., 2002) mutant mice. In both *Egfr*-null and *Dmm* mice, growth and development of Meckel's cartilage is affected, delaying the necessary forward movement of the mandible and tongue.

The mechanism by which the MES degrades to form a continuous mesenchymal palatal shelf has been a matter of intense debate. One proposal is that the loss of epithelial cells is caused by an epithelial-mesenchymal transition (EMT) (Fitchett and Hay, 1989). Although there is substantial data to suggest this process occurs in a portion of the cells in the MES, recent lineage tracing studies appear to rule out the possibility that these cells persist in the resulting mesenchymal core of the palate (Vaziri Sani et al., 2005). Alternate models propose that MES cells undergo apoptosis or migrate to either the oral or nasal epithelium. It is likely that a combination of these events leads to the eventual dissolution of the MES. During embryogenesis, the oral and nasal epithelium is bilayered, consisting of a cuboidal basal epithelial cell layer and a flattened, transient periderm layer on the surface (Fitchett and Hay, 1989). Current data suggest that, upon palatal shelf contact, periderm cells migrate toward accumulations of epithelial cells at the oral and nasal aspects of the shelf, where they undergo apoptosis (Carette and Ferguson, 1992; Cuervo and Covarrubias, 2004; Martinez-Alvarez et al., 2000b). Loss of the periderm layer has been proposed to be important for reinforcing the adhesion between the shelves mediated by the underlying basal cell layer (Fitchett and Hay, 1989; Nawshad et al., 2004).

Members of the Snail gene family play a central role in the patterning of vertebrate embryos. These genes drive epithelial-mesenchymal transitions throughout development by directly repressing the transcription of genes encoding components of cell-cell adhesive complexes in epithelia (Nieto, 2002). However,

The Jackson Laboratory, 600 Main Street, Bar Harbor, ME 04609, USA.

*Author for correspondence (e-mail: tom.gridley@jax.org)

Accepted 15 February 2007

members of the Snail gene family also have roles in other processes, such as the protection of cells from programmed cell death, the establishment of left-right asymmetry and the regulation of cell motility (reviewed by Barrallo-Gimeno and Nieto, 2005). Although at least some *Snai2*$^{-/-}$ mice are viable and fertile (Jiang et al., 1998b), they exhibit an interesting array of phenotypes, including an increased sensitivity in the hematopoietic lineages to induction of apoptosis by ionizing radiation (Inoue et al., 2002; Inukai et al., 1999). We have recently shown that conditional deletion of the *Snai1* gene in the epiblast results in randomization of left-right axis specification in mice (Murray and Gridley, 2006). Mutations of the *Snai1* and *Snai2* genes have also been shown to interact genetically with a *Twist1* mutation during the formation of cranial sutures (Oram and Gridley, 2005). Given these observations, we have extended our analysis of the functions of *Snai1* and *Snai2* genes during development of other craniofacial structures in mice, including the secondary palate. Here we report that approximately 50% of *Snai2*$^{-/-}$ mice present with cleft palate at birth, and the penetrance of this phenotype increases to 100% on a *Snai1* heterozygous background. Moreover, embryos with conditional deletion of the *Snai1* gene in neural crest cells on a *Snai2* null genetic background exhibit multiple craniofacial abnormalities, including defects such as micrognathia and cleft palate that are similar to those seen in Pierre Robin Sequence patients. These results demonstrate crucial roles for Snail gene family members in palatal shelf fusion and craniofacial morphogenesis in mice.

MATERIALS AND METHODS

Mice

The *Snai1*^{del1} (Carver et al., 2001) null allele, *Snai2*^{del1} and *Snai2*^{lacZ} null alleles (Jiang et al., 1998b), and *Snai1*^{flox} conditional allele (Murray et al., 2006) have been described previously. *Snai1*$^{flox/flox}$ mice were maintained as homozygotes and bred to *Snai2*$^{+/-}$ mice for the experiments described in this report. *Wnt1-Cre* mice (Danielian et al., 1998) were obtained from the Jackson Laboratory. Typically, compound heterozygous mice carrying *Snai1* and *Snai2* null alleles were bred to single heterozygous *Snai2* female mice to generate *Snai1*$^{+/-}$ *Snai2*$^{-/-}$ and *Snai1*$^{+/+}$ *Snai2*$^{-/-}$ progeny. Similarly, male mice harboring *Wnt1-Cre*, *Snai1* and *Snai2* alleles were crossed to *Snai1*$^{flox/flox}$ *Snai2*$^{+/-}$ females, and embryos were isolated at varying gestational stages. Embryos of the genotype *Wnt1-Cre*/+ *Snai1*$^{flox/-}$ are designated *Snai1* conditional knockout (*Snai1-cko*), while those also null for *Snai2* are designated *Snai1/2* double knockout (*Snai1/2-dko*). ROSA26-EGFP mice (Mao et al., 2001) containing a Cre-inducible GFP reporter in the ROSA26 locus were obtained from the Jackson Laboratory. The ROSA26-EGFP mice were bred to *Wnt1-Cre*/+ *Snai1*$^{flox/flox}$ *Snai2*$^{+/-}$ mice and subsequently bred to homozygosity for the ROSA26-EGFP reporter and *Snai1*^{flox} alleles. Embryos or neonatal mice were genotyped by allele-specific PCR of DNA isolated from the yolk sac or tail.

In situ hybridization

Radioactive in situ hybridization was performed essentially as described (Krebs et al., 2001), except ^{33}P-UTP was used instead of ^{35}S as the labeled nucleotide. Exposure times for each probe were determined empirically. Radioactive probes were made using the Promega (Madison, WI) Riboprobe kit, using ^{33}P-labeled UTP (Perkin-Elmer, Waltham, MA). Whole-mount in situ hybridization was performed as described (Krebs et al., 2001), and digoxigenin-labeled riboprobes were generated using the Roche (Indianapolis, IN) labeling kit according to the manufacturer's instructions.

Histology and immunostaining

Histology, immunohistochemistry and immunofluorescence were performed on 7 μm sections of paraformaldehyde-fixed, paraffin-embedded embryos. Antibodies for keratin 6 (Clone LHK6B, NeoMarkers, Fremont, CA) and phospho-histone H3 (Upstate Biotechnology, Charlottesville, VA) were diluted 1:100 in 4% goat serum/PBS. Quantitation of phospho-histone H3 staining was performed by counting equivalent areas of eight separate sections from two embryos for each age/genotype. Data is presented as the mean±s.e.m., and *P*-values were computed using Student's *t*-test. An antigen retrieval step comprising boiling for 10 minutes in 10 mM citric acid was performed for both antibodies. For keratin 6, an Alexa Fluor 488-labeled secondary antibody (Invitrogen, Carlsbad, CA) was used at a 1:400 dilution and samples were counterstained with Hoescht 33342 (Invitrogen, Carlsbad, CA) and mounted using Vectashield hard set mounting media (Vector Labs, Burlingame, CA). Phospho-histone H3 staining was visualized using diaminobenzidine (DAB) following incubation with a peroxidase conjugated secondary antibody (Jackson ImmunoResearch, West Grove, PA) diluted to 1:2000. EGFP was visualized by immunostaining with a chicken anti-GFP antibody (Aves Labs, Tigard, OR) and Alexa Fluor 488-conjugated anti-chicken secondary antibodies. For TUNEL analysis, samples were analyzed using the In Situ Cell Detection Kit, Fluorescein (Roche, Indianapolis, IN). Coronal cryostat sections of embryonic day 14.5 (E14.5) *Snai2*^{lacZ} embryos were stained for β-galactosidase activity, as described (Oram et al., 2003).

Skeletal staining

Newborn mutant mice and littermate controls were stained with Alcian Blue and Alizarin Red to visualize skeletal and cartilaginous elements. Embryos were skinned, eviscerated and fixed overnight in 100% ethanol (EtOH). They were then stained overnight in 0.015% Alcian Blue, 0.005% Alizaran Red in 5% acetic acid/70% EtOH. Clearing was performed in 1% potassium hydroxide/20% glycerol, after which they were brought into 100% glycerol for photography and storage. A modification of this method omitting the Alizarin Red was used to visualize the cartilaginous skeleton of E14.5 embryos. Embryos were then washed in 70% EtOH and cleared in 1:2 benzyl alcohol:benzyl benzoate.

Electron microscopy

Mandibles of E14.5 and E17.5 embryos were removed to visualize the palate, and the embryos were fixed at 4°C with 2.5% glutaraldehyde in 0.1 M sodium cacodylate, pH 7.4. Following washes, embryos were post-fixed in 1% osmium tetroxide in 0.1 M sodium cacodylate for 2 hours at 4°C, dehydrated and dried under CO_2. Samples were then mounted, sputter coated with gold to 15 nm, and examined at 20 kV with a Hitachi 3000N scanning electron microscope.

RESULTS

Cleft palate in *Snai2*$^{-/-}$ and *Snai1*$^{+/-}$ *Snai2*$^{-/-}$ neonatal mice

We have described previously construction of targeted null alleles of the *Snai1* and *Snai2* genes, including a *Snai2*^{lacZ} targeted knock-in allele (Carver et al., 2001; Jiang et al., 1998b). Observation of the progeny of *Snai2*$^{+/-}$ intercrosses after birth revealed a striking reduction in the number of *Snai2*$^{-/-}$ mice at weaning. When observed shortly after birth, some *Snai2*$^{-/-}$ progeny presented with severe abdominal distention from air accumulation and absence of milk in the stomach, both due to cleft secondary palate. Further analysis revealed that approximately 50% of *Snai2*$^{-/-}$ neonates presented with cleft palate. Penetrance of cleft palate increased to 100% in *Snai1*$^{+/-}$ *Snai2*$^{-/-}$ neonatal mice, revealing functional redundancy between these two gene family members (Fig. 1A,B). Histological analysis revealed that the palatal shelves of *Snai1*$^{+/-}$ *Snai2*$^{-/-}$ embryos at E15.0 elevated normally and came into contact at the midline (Fig. 1C,D). However, the shelves failed to form an MES and fuse. It is likely that the subsequent growth of the head caused separation of the unfused palatal shelves, resulting in the cleft secondary palate observed at birth.

To better understand the potential roles of the *Snai1* and *Snai2* genes in palate development, we analyzed and compared their expression patterns during palatogenesis. *Snai1* gene expression was assessed by in situ hybridization, while *Snai2* expression was determined by β-galactosidase expression of the *Snai2*^{lacZ} allele

(Jiang et al., 1998b). At E13.5, the *Snai1* gene was expressed throughout the palatal shelf mesenchyme, with particularly high levels in the cells underlying the MEE at the anterior and along the medial aspect of the shelf mesenchyme at the posterior (Fig. 1E,F). At E14.5, strong expression was observed in the palatal mesenchyme just adjacent to the newly formed MES (Fig. 1G,H), consistent with a previous report (Martinez-Alvarez et al., 2004). *Snai2* expression at E14.5 was more diffuse, but was present throughout the palate mesenchyme and epithelium (Fig. 1I,J). Interestingly, we noted an enhancement of β-galactosidase expression from the $Snai2^{lacZ}$ allele on a $Snai1^{+/-}$ heterozygous genetic background (Fig. 1J versus 1I), suggesting that a compensatory mechanism regulating gene expression levels may exist between these two genes.

Marker expression in $Snai2^{-/-}$ and $Snai1^{+/-}$ $Snai2^{-/-}$ palates

Substantial work has implicated transforming growth factor β gene family members in palate development. Targeted deletion of the *Tgfb3* gene results in cleft palate in mice (Kaartinen et al., 1995), and mutations in the *Tgfb3* gene have been associated with nonsyndromic cleft palate in humans (Lidral et al., 1998). The palatal shelves of *Tgfb3*-null mice grow, elevate and meet at the midline normally but fail to adhere and fuse (Kaartinen et al., 1995; Taya et al., 1999). This is consistent with the expression pattern of the *Tgfb3* gene along the MEE, and is very similar to the phenotype of $Snai2^{-/-}$ and $Snai1^{+/-}$ $Snai2^{-/-}$ mice at E14.5. Therefore, we examined whether alterations in *Tgfb3* expression could explain the phenotypes observed in $Snai2^{-/-}$ and $Snai1^{+/-}$ $Snai2^{-/-}$ mice. However, expression of the *Tgfb3* gene was unaltered in either $Snai2^{-/-}$ or $Snai1^{+/-}$ $Snai2^{-/-}$ embryos (Fig. 2A-C). Similarly, the *Irf6* gene, which is mutated in some human cleft palate patients and is expressed throughout the palatal shelf epithelium (Knight et al., 2006; Kondo et al., 2002), was expressed normally in $Snai2^{-/-}$ and $Snai1^{+/-}$ $Snai2^{-/-}$ mutant embryos (Fig. 2D-F).

Palatal shelf adhesion and fusion requires a series of modifications in the morphology and expression of cell surface proteins of the MEE. As the shelves approach each other, periderm cells along the apical surface of the MEE bulge and extend filopodia and lamellipodia from their surface (Martinez-Alvarez et al., 2000a; Taya et al., 1999). In *Tgfb3* mutant mice, these cellular movements are defective and the shelves subsequently fail to adhere. Although *Tgfb3* expression appeared normal in $Snai1^{+/-}$ $Snai2^{-/-}$ mutants, it is possible that *Snai1* and *Snai2* function lies downstream of TGFβ3 function. Scanning electron microscopy revealed that both control and $Snai1^{+/-}$ $Snai2^{-/-}$ palatal shelves exhibited the normal presence of both bulging cells and lamellipodia on the MEE of E14.5 embryos (Fig. 3A,B). Numerous studies have highlighted the importance of apoptosis in palatal shelf fusion (Carette and Ferguson, 1992; Cuervo and Covarrubias, 2004; Martinez-Alvarez et al., 2000b). Along with their described roles in regulating EMT, the *Snai1* and *Snai2* genes also have been demonstrated to regulate apoptosis (Inoue et al., 2002; Inukai et al., 1999; Vega et al., 2004). Therefore, we examined whether there were any alterations in apoptosis in the developing palate of $Snai1^{+/-}$ $Snai2^{-/-}$ mutant embryos at E14.5. Control embryos displayed substantial apoptosis along the MES (Fig. 3E, arrowheads), concentrated at the oral and nasal aspects of the seam in accumulations of epithelial cells termed epithelial triangles (Fig. 3C,E, arrows). In mutant embryos, however, we observed a dramatic reduction in the number of apoptotic cells at the intersection of the two palatal shelves, suggesting that failure to undergo normal programmed cell death might account for the cleft palate phenotype in $Snai1^{+/-}$ $Snai2^{-/-}$ mutants (Fig. 3D,F). Although an occasional TUNEL-positive cell along the MEE of mutant shelves was observed, comprehensive analysis of these embryos (n=4, at least 20 sections per embryo along the anteroposterior axis) revealed that this was a rare event. Indeed, apoptosis of periderm cells has been observed before MES formation, prompting the suggestion that removal of the periderm

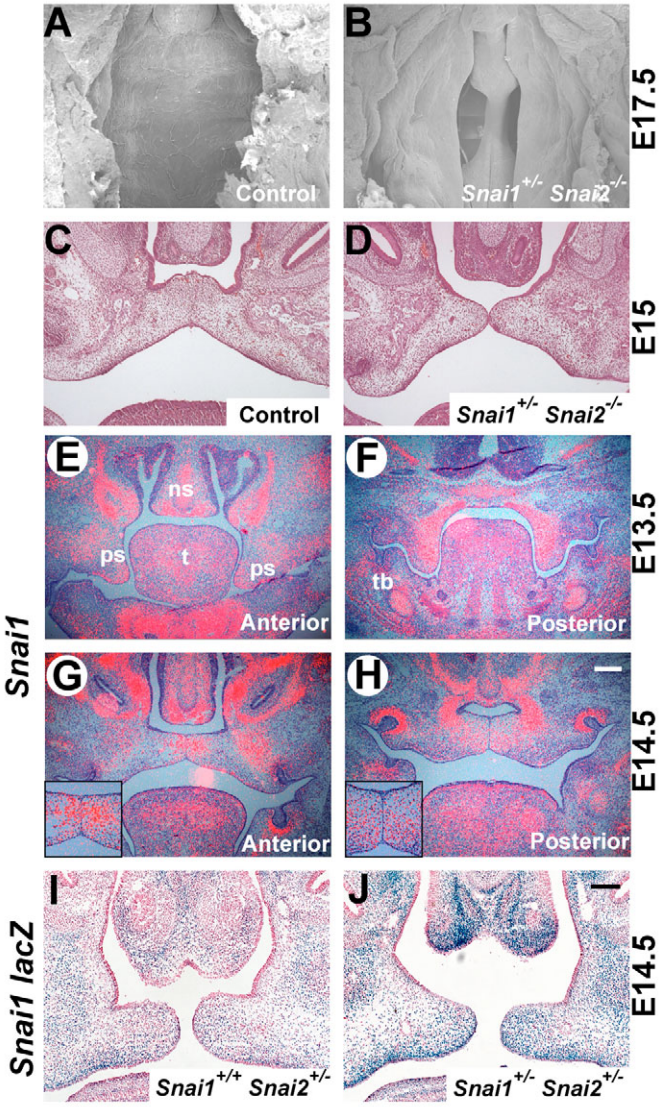

Fig. 1. The *Snai1* and *Snai2* genes are essential for palate development. (**A**,**B**) Scanning electron micrographs showing cleft secondary palate at E17.5 in $Snai1^{+/-}$ $Snai2^{-/-}$ mutant embryos. (**C**,**D**) Coronal sections at E15 showing the fused secondary palate in control embryos (C), and the adjacent, but unfused palatal shelves in $Snai1^{+/-}$ $Snai2^{-/-}$ mutant embryos (D). (**E-H**) Expression of the *Snai1* gene in the developing palate of E13.5 and 14.5 embryos. Note the expression in the palatal shelf mesenchyme at each stage and the strong expression adjacent to the MES at E14.5 (inset). (**I**,**J**) *Snai2* expression, detected by β-galactosidase activity of the $Snai2^{lacZ}$ allele, showing widespread expression in the palatal shelf mesenchyme and nasal/oral epithelia. Note the increase in β-galactosidase activity in mice with deletion of a single *Snai1* allele (J). ns, nasal septum; ps, palatal shelf; t, tongue; tb, tooth bud. Scale bar: 100 μm in C,D,I,J; 200 μm in E-H.

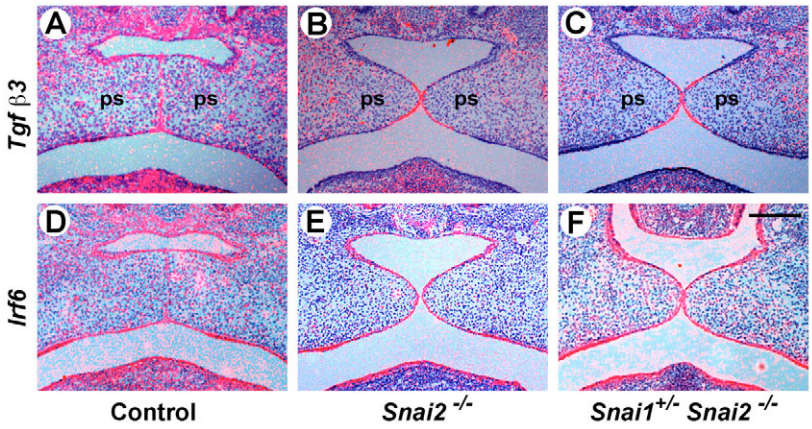

Fig. 2. Expression of the *Tgfb3* and *Irf6* genes is unaffected in *Snai2*$^{-/-}$ and *Snai1*$^{+/-}$ *Snai2*$^{-/-}$ palates at E14.5. (**A-C**) In situ hybridization showing expression of *Tgfb3* along the MES of control embryos and clear expression at the adjacent but unfused MEE of mutant embryos. (**D-F**) The *Irf6* gene is expressed throughout the oral and nasal epithelia in both control and mutant embryos. ps, palatal shelf. Scale bar: 200 μm.

is necessary for adhesion (Fitchett and Hay, 1989). Countering this model is the observation using cell surface labeling techniques that periderm cells migrate toward the epithelial triangles after adhesion, where they undergo extensive apoptosis (Cuervo and Covarrubias, 2004). Thus, it is likely that a combination of migration to epithelial triangles and apoptosis are required for the proper formation of the MES per se, a structure that is not formed in *Snai1*$^{+/-}$ *Snai2*$^{-/-}$ mutant embryos. Periderm cells marked by expression of keratin 6 (Mazzalupo and Coulombe, 2001) were observed migrating into the epithelial triangles of control embryos (Fig. 3G), while in mutant embryos (Fig. 3H) keratin 6-expressing cells were confined to a discrete domain along the medial aspect of the adjacent palatal shelves. Just before fusion, K6-positive cells were present on the medial aspects of the palatal shelves of both control and mutant embryos (data not shown). Migration of periderm cells is thought to play an important role in epithelial fusions (Mazzalupo and Coulombe, 2001), and a defect in periderm cell migration thus represents a logical explanation, along with a concomitant reduction in apoptosis, for the fusion defect observed in *Snai1*$^{+/-}$ *Snai2*$^{-/-}$ mutant palates.

Conditional deletion of the *Snai1* gene in neural-crest-derived cells does not cause craniofacial defects

Although *Snai1*$^{+/-}$ *Snai2*$^{-/-}$ mutant mice exhibit palate defects that apparently result from a failure of MEE fusion, its expression pattern suggested a possible role for the *Snai1* gene in the mesenchymal component of the palatal shelf. As the early lethality of *Snai1*$^{-/-}$ embryos precludes examination of the role of this gene in palate development, we employed a conditional *Snai1*^{flox} allele (Murray et al., 2006). We used the *Wnt1-Cre* line (Danielian et al., 1998) to delete the *Snai1* gene in palatal shelf mesenchyme, because an earlier study had shown *Wnt1-Cre* to be an effective deleter in the vast majority of palatal mesenchyme cells (Ito et al., 2003). Although the *Snai1* gene has been proposed to play an important role in the formation of the neural crest, we have shown that, surprisingly, *Snai1* function is not required for neural crest cell delamination and migration through E9.5 in mice (Murray and Gridley, 2006). Thus, this approach permitted us to test both the role of the *Snai1* gene in palatal shelf growth and fusion and its role in the development of neural-crest-derived structures after E9.5. In order to determine the effectiveness of *Snai1* deletion in the appropriate cell types, we analyzed *Snai1* expression by whole-mount in situ hybridization. *Snai1* expression in the branchial arches was completely lost in *Wnt1-Cre Snai1*$^{flox/-}$ (designated *Snai1-cko*) embryos by E9.5 (Fig. 4A,B). Surprisingly, the *Snai1-cko* mice were viable, fertile and exhibited no obvious phenotypic abnormalities (data not shown).

Redundant function of the *Snai1* and *Snai2* genes in cranial neural crest cells

As we did not observe any obvious phenotypic abnormalities in *Snai1-cko* mice, we bred the *Snai2*$^{+/-}$ allele into this cross and examined the effects of compound mutant alleles on palate development. We observed the expected frequencies of cleft palate in *Snai2*$^{-/-}$ and *Snai1*$^{+/-}$ *Snai2*$^{-/-}$ mice. However, *Wnt1-Cre Snai1*$^{flox/-}$ *Snai2*$^{-/-}$ mice (hereafter designated *Snai1/2-dko*) exhibited an extensive array of craniofacial defects, including cleft palate. We observed a striking difference in the phenotype of the developing palate in *Snai1/2-dko* embryos compared with *Snai1*$^{+/-}$ *Snai2*$^{-/-}$ embryos. Rather than elevating normally and failing to fuse, as the palatal shelves of *Snai1*$^{+/-}$ *Snai2*$^{-/-}$ embryos did, the palatal shelves of *Snai1/2-dko* embryos remained in their vertical growth orientation and failed to elevate (Fig. 4C,D). Other craniofacial defects observed in *Snai1/2-dko* neonates included presence of an abnormal mandible that was significantly shorter than that of control mice (Fig. 4E,F). The mandible of the *Snai1/2-dko* neonates appeared to be missing the rostral portion of the Meckel's cartilage and was fused at the midline (Fig. 4G,H). In addition, *Snai1/2-dko* mice had a dome-shaped skull, shortened parietal bones and an enlarged frontal foramen (Fig. 4I,J). This spectrum of defects is also seen in mice with mutations in neural crest regulatory genes such as *Alk2* (*Acvr1* – Mouse Genome Informatics) (Dudas et al., 2004), *AP-2a* (*Tcfap2a* – Mouse Genome Informatics) (Brewer et al., 2004) and *Tgfbr2* (Ito et al., 2003). Our results demonstrate that although the *Snai1* and *Snai2* genes play no detectable role in the early generation and emigration of the mouse neural crest (Murray and Gridley, 2006), these genes are important for proper differentiation and patterning of cranial neural-crest-derived structures.

Marker expression in *Snai1/2-dko* palates

One possible cause for the arrest in palate development before shelf elevation is disruption in the normal growth and/or patterning of the developing shelves. To examine this hypothesis, we analyzed the expression of genes known to play important roles in palate development before shelf fusion. The paired class homeodomain transcription factor Pax9 is crucial for proper palatal shelf patterning, and *Pax9*-null mice display impaired palatal shelf elevation (Peters et al., 1998). At E13.5, the *Pax9* gene is expressed in the palatal shelf mesenchyme and in the condensing mesenchyme surrounding the developing molars (Fig.

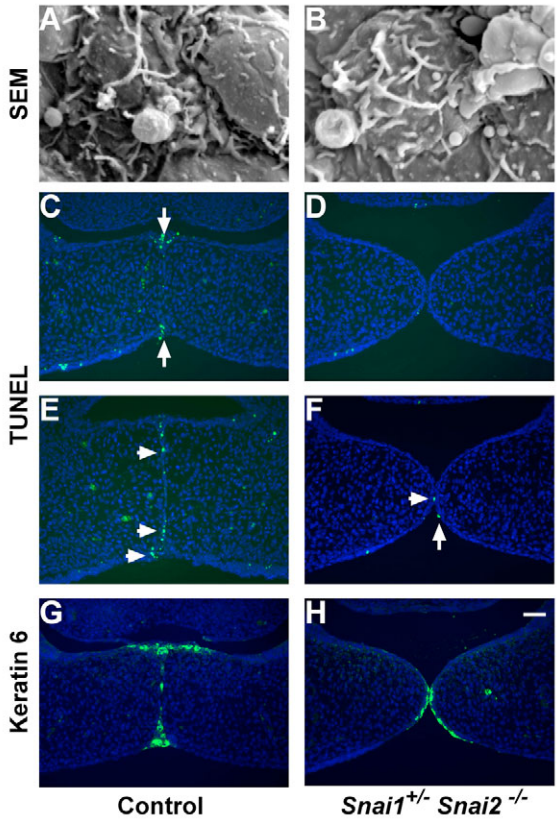

Fig. 3. *Snai1*$^{+/-}$ *Snai2*$^{-/-}$ palatal shelves display reduced apoptosis and defective periderm migration. (**A**,**B**) Scanning electron micrographs of the MEE of control (A) and *Snai1*$^{+/-}$ *Snai2*$^{-/-}$ mutant (B) embryos at E14.5. Samples were dissected just before palatal shelf fusion, when shelves were in close approximation. Note the appearance of lamellipodia on the MEE of both control and mutant embryos. (**C-F**) TUNEL staining showing apoptosis along the MES (E) and in the epithelial triangles (C,E) of control embryos at E14.5, whereas mutant embryos (D,F) lack any detectable cell death along the MEE. Arrows, epithelial triangles; arrowheads, MES. (**G**,**H**) Keratin 6 immunofluorescence marking periderm cells at the palate fusion point in control embryos at E14.5. Note the concentration of periderm cells in the epithelial triangles in the control embryo, with occasional remaining cells in the MES (G). Mutant palates, in contrast, show the presence of periderm cells at the junction of the adjacent shelves without the formation of epithelial triangles (H). Scale bar: 50 μm.

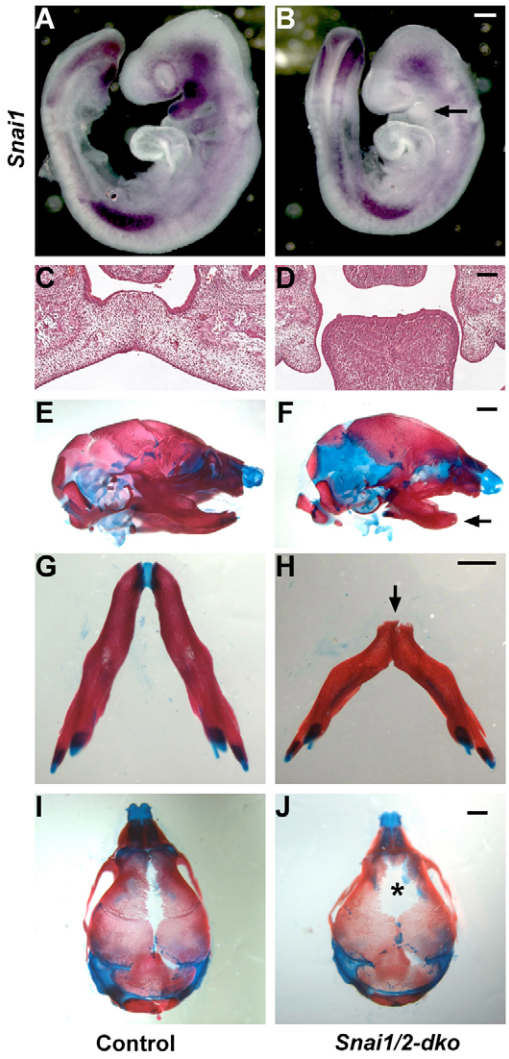

Fig. 4. Cleft palate and craniofacial abnormalities in *Snai1/2-dko* mice. (**A**,**B**) Whole-mount in situ hybridization for *Snai1* of E9.5 control and *Snai1-cko* embryos showing effective deletion of *Snai1* by *Wnt1-Cre* in the neural crest. Note the absence of *Snai1* expression in the first branchial arch (arrow in B) in the mutant embryo versus control. (**C**,**D**) Histology of the cleft palate in *Snai1/2-dko* embryos, showing the vertically oriented palatal shelves in mutant embryos. (**E**,**F**) Skulls of *Snai1/2-dko* mice are smaller, dome-shaped, and have a shortened mandible (arrow). (**G**,**H**) Ventral view of the mandible of control (G) and mutant (H) neonates. Note the overall shorter length, missing rostral Meckel's cartilage and midline fusion (arrow) in the mutant. (**I**,**J**) An enlarged frontal foramen (asterisk) is apparent in the *Snai1/2-dko* neonate. Scale bar: 200 μm in A,B; 100 μm in C,D; 2 mm in E,F; 1 mm in G-J.

5A), and a similar pattern was observed in *Snai1/2-dko* embryos at both E13.5 and 14.5 (Fig. 5B,C). Similarly, no difference between control and mutant embryos was noted in the expression of the *Msx1* gene (Fig. 5D-F), which is crucial for normal growth of the anterior palatal shelves (Zhang et al., 2002). Expression of the *Shh* gene is dynamic in the developing palate, and is restricted to a small domain of thickened oral epithelium at E13.5 (Fig. 5G), where it plays a role in providing a mitogenic signal to the adjacent mesenchyme. In *Fgf10*$^{-/-}$ and *Fgfr2*$^{-/-}$ mice, *Shh* expression is disrupted, concomitant with a decrease in proliferation in the nascent palatal shelves (Rice et al., 2004). In *Snai1/2-dko* mice, the *Shh* gene was expressed in the proper domain at both stages, but at a somewhat reduced intensity (Fig. 5H,I). The *Osr1* gene is expressed in a dynamic mediolateral pattern in the developing palatal shelf and has been suggested to play an important role in palatal shelf patterning (Lan et al., 2004). Control embryos displayed *Osr1* expression in the lateral aspects of the vertical palatal shelf (Fig. 5J), while staining in *Snai1/2-dko* mutant shelves at E13.5 and 14.5 was reduced somewhat, although some expression was noted in the proper domains (Fig. 5K,L). Given the role of the *Shh* gene in regulating cell division (Ingham and McMahon, 2001), we analyzed cell proliferation in control and mutant embryos using a marker of mitosis, phospho-histone H3. When compared to an equivalent area of E13.5 control palatal shelves (78.4±10), we could not detect any significant changes in the numbers of mitotic cells in

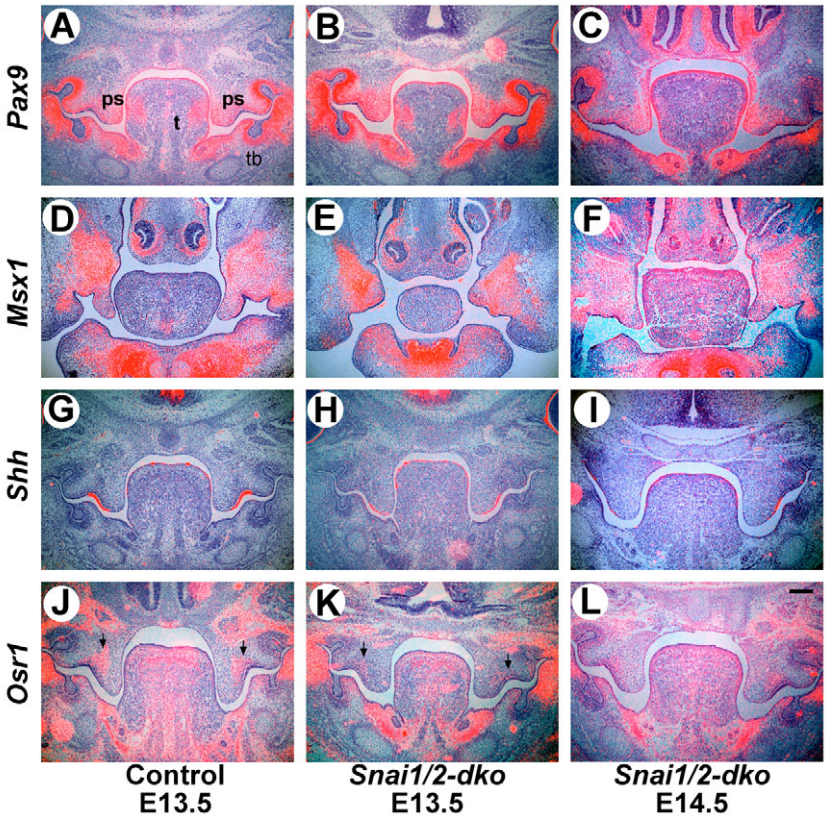

Fig. 5. Expression of markers of palate development in *Snai1/2-dko* embryos. (**A-C**) At E13.5, *Pax9* is expressed in a dynamic pattern, transitioning from the lateral to medial aspects of the palatal shelf. Both control and mutant embryos show similar expression of an intermediate pattern (A,B), while E14.5 mutant shelves show the full transition to medial expression in the posterior palate (C). (**D-F**) *Msx1* expression at E13.5 is normally restricted to the anterior palatal shelf mesenchyme. Expression of *Msx1* appears unaltered in mutant shelves at E13.5 and in the vertically oriented E14.5 shelves. (**G-I**) *Shh* expression at E13.5 is localized to the thickened oral epithelium lateral to the vertical palatal shelf. Mutant embryos display the proper pattern at both stages, but the expression level appears somewhat reduced. (**J-L**) At E13.5 *Osr1* is expressed in discrete domains in the lateral palatal shelf mesenchyme (arrows). As with *Shh*, note the proper patterning, but reduced expression, in mutant embryos. ps, palatal shelf; t, tongue; tb, tooth bud. Scale bar: 200 μm.

Snai1/2-dko palatal shelves at either E13.5 (80.2±10, P=0.28) or E14.5 (85.5±15, P=0.15) (Fig. 6). Thus, the subtle change in *Shh* expression observed in *Snai1/2-dko* mice does not appear to result in any major perturbation of the proliferative potential of the developing palatal shelves. These results demonstrate that there are no major disruptions in *Snai1/2-dko* mutants in the expression of several genes central to the control of palatal shelf patterning.

Another explanation for the phenotype observed in *Snai1/2-dko* embryos is a defect in the migration and subsequent population of neural crest cells in craniofacial structures. Although we have shown previously that neither the *Snai1* gene nor the *Snai2* gene plays an essential role in the delamination and initial migration of neural crest cells (Murray and Gridley, 2006), we performed lineage-tracing analyses on E11.5, 12.5 and 14.5 embryos utilizing ROSA26-EGFP reporter mice (Mao et al., 2001). We observed no obvious differences in the distribution of EGFP-labeled cells in *Snai1/2-dko* embryos at any of these stages (see Fig. S1 in the supplementary material), indicating that there are no major disruptions of neural crest cell migration in *Snai1/2-dko* embryos. It is notable that subtle differences in the size and shape of the anterior palatal shelves were observed in some *Snai1/2-dko* mutants (Fig. 5E, Fig. 6D; see Fig. S2 in the supplementary material). These differences were apparent in only a subset of *Snai1/2-dko* mutant embryos (see Fig. S2 in the supplementary material), as there appears to be considerable variability in the extent of outgrowth in control anterior palatal shelves (see Fig. S2A versus S2C in the supplementary material). Although we did not observe any differences in cell proliferation between control and mutant embryos, we cannot exclude the possibility that delayed outgrowth of the anterior palatal shelves plays a role in the cleft palate phenotype of *Snai1/2-dko* embryos.

Cleft palate in *Snai1/2-dko* mice is probably secondary to defects in mandible development

As patterning and growth of the palatal shelves in *Snai1/2-dko* mice appeared to be essentially normal, we examined whether the palatal shelf defects might be secondary to the craniofacial defects noted at birth. Mandibular malformations, such as micrognathia, are proposed to be the underlying cause of cleft palate in several mouse mutants, such as *Egfr*$^{-/-}$ (Miettinen et al., 1999), *Hoxa2*$^{-/-}$ (Gendron-Maguire et al., 1993) and *Dmm* (Ricks et al., 2002) mutant mice. Because the forward growth of the mandible driven by the extension of the neural-crest-derived Meckel's cartilage provides the mechanism to lower the tongue and permit palatal shelf elevation, any defects in this process could result in a cleft palate phenotype similar to that observed in *Snai1/2-dko* mice. In light of the mandibular abnormalities observed at birth (Fig. 4F,H), we performed Alcian Blue staining of the embryonic cartilage at E14.5 to determine if defects in Meckel's cartilage could be observed at this crucial time point. Meckel's cartilage was dramatically shorter in *Snai1/2-dko* embryos compared with control embryos (Fig. 7). Therefore, we propose that that the underlying cause of cleft palate in *Snai1/2-dko* embryos is abnormal development of Meckel's cartilage, which in turn prevents the normal extension of the tongue and elevation of the palatal shelves.

DISCUSSION

Redundant *Snai1* and *Snai2* gene function during palatal shelf fusion

This study describes multiple roles for the Snail family genes *Snai1* and *Snai2* during palate development and craniofacial morphogenesis in mice. Our data suggest a role for the *Snai2* gene in formation of the MES and/or palatal shelf adhesion. Modulation of the penetrance of this phenotype by reduction of *Snai1* gene

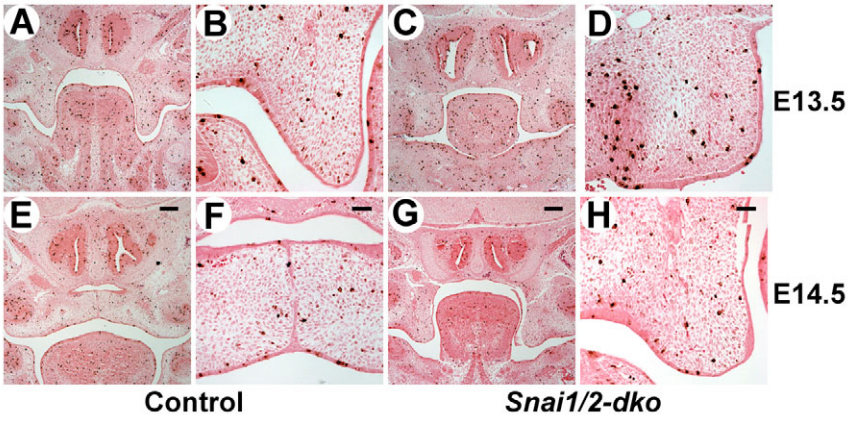

Fig. 6. Similar levels of cell proliferation in control and *Snai1/2-dko* palatal shelves. Phospho-histone H3 immunostaining of E13.5 (**A-D**) and E14.5 (**E-H**) palates showing a similar number of mitotic cells in control (A,B,E,F) and *Snai1/2-dko* (C,D,G,H) embryos. Note the vertical positioning of the mutant palate shelf at E14.5 (H). Scale bar: 200 μm in A,C,E,G; 50 μm in B,D,F,H.

dosage supports the notion that these genes have redundant roles in vivo, consistent with our observations that *Snai2*^{lacZ} expression increases on a *Snai1*$^{+/-}$ genetic background. We also demonstrate a genetic interaction between mutations in the *Snai1* and *Snai2* genes in the formation of neural-crest-derived craniofacial structures. The co-expression and genetic interaction clearly demonstrate functional redundancy and compensatory activity between the *Snai1* and *Snai2* genes.

Martinez-Alvarez et al. (Martinez-Alvarez et al., 2004) previously described high levels of *Snai1* gene expression in palatal shelf mesenchyme, and noted that a few MES cells express the *Snai1* gene during the fusion process, thus supporting a small role for EMT in MES dissolution. Interestingly, they also observed a dramatic increase in *Snai1* expression in the MES of *Tgfb3*$^{-/-}$ mutant palates, and proposed a model in which increased compensatory expression of the *Tgfb1* gene induces *Snai1* expression, thereby protecting these cells from apoptosis (Barrallo-Gimeno and Nieto, 2005; Vega et al., 2004). This suggests a model in which the *Snai1* gene plays an important role in regulating the survival of MEE and MES cells. We did not observe an increase in apoptosis in the mutant palatal shelves, but instead observed a complete absence of cell death. This might be secondary, however, to a more fundamental defect in palatal shelf fusion. In support of this notion, we find that periderm cells remained at the intersection of the two MEE layers, and did not migrate toward the oral and nasal epithelia.

Defects in MES formation in *Snai1*$^{+/-}$ *Snai2*$^{-/-}$ mice

A crucial component of palate development is the adhesion of the palatal shelves and subsequent transformation of the separate MEE into a single MES (Ferguson, 1988). Normally, as the palatal shelves approach each other, periderm cells of the bilayered MEE bulge, form lamellipodia and express extracellular matrix proteins important for adhesion on their surface. After contact is initiated, periderm cells migrate to the oral and nasal aspects of the forming MES and undergo apoptosis (Cuervo and Covarrubias, 2004). The basal epithelial cells intercalate to form a single layer MES, which then disappears as the basal cells also commit to an apoptotic program. Several mouse models of cleft palate exhibit defects in this process, the classic example being the *Tgfb3*-null mouse (Kaartinen et al., 1995; Taya et al., 1999). In these embryos, palatal shelves elevate normally, but periderm cells fail to bulge and do not form lamellipodia. Our results show that *Snai1*$^{+/-}$ *Snai2*$^{-/-}$ mutant embryos display normal expression of the *Tgfb3* gene and the presence of bulging cells and lamellipodia on the surface of the MEE. However, our data demonstrate that *Snai1*$^{+/-}$ *Snai2*$^{-/-}$ embryos lack both the apoptosis normally observed at the MES and the migration of periderm cells to form epithelial triangles. It had been suggested that cell death of the periderm layer is crucial for the proper intercalation and adhesion of the underlying basal cell layer (Fitchett and Hay, 1989). However, in vitro labeling experiments show that a substantial portion of the periderm migrates to epithelial triangles at the nasal and oral aspects of the MES (Carette and Ferguson, 1992), where they then undergo apoptosis (Cuervo and Covarrubias, 2004; Cuervo et al., 2002). Thus, a model emerges wherein adhesion stimulates migration of the periderm, which in turn allows for intercalation of the basal epithelial cells and formation of the mature MES. One prediction from this model is that defects in periderm cell migration would short-circuit the program and result in a lack of periderm cell death and basal cell intercalation. Our data are consistent with a failure of periderm cell migration in *Snai1*$^{+/-}$ *Snai2*$^{-/-}$ mutants. The absence of apoptosis could then be attributed to the persistence of the periderm on the MEE.

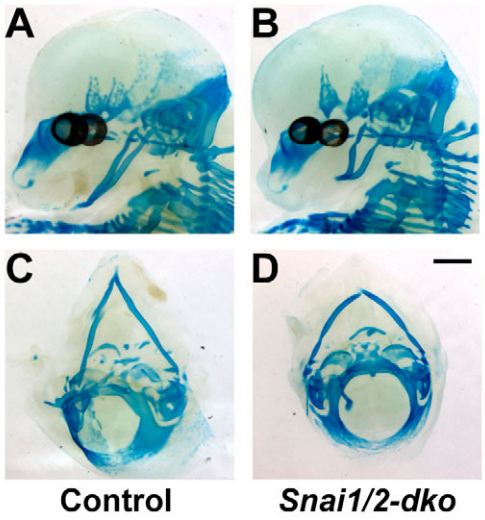

Fig. 7. Defects in Meckel's cartilage extension in *Snai1/2-dko* embryos. Alcian Blue staining of control and mutant embryos at E14.5, showing the dramatically reduced extension of the Meckel's cartilage. (**A**,**B**) Lateral views. (**C**,**D**) Ventral views. Scale bar: 1 mm.

Could a failure to undergo EMT following MEE adhesion contribute to the cleft palate phenotype of *Snai1*$^{+/-}$ *Snai2*$^{-/-}$ embryos? Using fate-mapping analysis, Vaziri Sani et al. claimed that the absence of persistently labeled cells in the palatal shelf mesenchyme precluded EMT as a possible mechanism for palatal shelf fusion (Vaziri Sani et al., 2005). However, the data presented did not address whether MES cells could be observed undergoing EMT at the early stages of fusion, only that they did not ultimately contribute to the mesenchymal core. It is possible that EMT might occur in cells fated to undergo apoptosis, thus escaping identification in fate-mapping studies. Indeed, the migration of periderm cells presumably requires modification of their epithelial phenotype in order to migrate toward the epithelial triangles. Thus, it remains plausible that EMT is occurring at some point during the process of MES dissolution, although these cells ultimately do not contribute in a long-term manner to the palate mesenchyme.

Functions of Snail family genes in mouse neural crest development

We have reported previously the surprising result that neither the *Snai1* nor the *Snai2* gene, alone or in combination, is required for neural crest cell generation and delamination in mice, at least through 9.5 days of gestation (Murray and Gridley, 2006). It had been widely proposed that the *Snai1* gene would play an essential role in neural crest delamination in mice, based on the observations that: (1) *Snai1* is expressed in the dorsal neural folds concomitant with neural crest cell delamination (Locascio et al., 2002; Sefton et al., 1998); (2) ectopic *Snai1* gene expression induces EMT in cultured epithelial cells (Batlle et al., 2000; Cano et al., 2000); (3) the *Snai2* gene plays a crucial role in neural crest cell delamination in the chick (Nieto et al., 1994); (4) *Snai2*$^{-/-}$ mice lack an obvious neural crest phenotype (Jiang et al., 1998b); and (5) the *Snai1* and *Snai2* genes are expressed in a modular fashion across vertebrate species (Locascio et al., 2002). The results presented here reveal an entirely different role for the *Snai1* and *Snai2* genes in craniofacial morphogenesis. While loss of a single *Snai1* allele in the context of a *Snai2*-null background (*Snai1*$^{+/-}$ *Snai2*$^{-/-}$ mice) results in palatal clefting due to defects in periderm cell migration and apoptosis, removing the remaining *Snai1* allele in the neural crest (*Snai1/2-dko* mice), which populates a majority of the palatal shelf mesenchyme, results in a very different cleft palate phenotype. Marker analysis revealed only very subtle alterations in palatal shelf patterning, including a small but clear decrease in the expression of *Shh* in the oral epithelium and *Osr1* in the mesenchyme. Indeed, these changes may be related to the apparent small differences in anterior palatal shelf outgrowth observed in *Snai1/2-dko* embryos compared to some controls. It is unlikely, however, that these changes are ultimately responsible for the observed cleft palate phenotype. In addition to cleft palate, *Snai1/2-dko* embryos also exhibit other craniofacial abnormalities, including micrognathia, fused mandible and an enlarged parietal foramen in the skull vault. This combination of phenotypes has been observed in other conditional neural crest mutants, such as *Alk2* (Dudas et al., 2004), *AP-2a* (Brewer et al., 2004) and *Tgfbr2* (Ito et al., 2003), and demonstrates that although the *Snai1* and *Snai2* genes are not essential in the initial delamination and migration of neural crest cells from the neural tube, they play a crucial role in the later development of neural-crest-derived structures.

Snai1/2-dko embryos as a model for Pierre Robin Sequence

The Pierre Robin Sequence (also termed Robin Sequence) is a human developmental malformation characterized by mandibular retrognathia (normal size receded mandible) or micrognathia (abnormally small mandible), glossoptosis (rearward and downward displacement of the tongue) and cleft palate. Most newborns with Pierre Robin Sequence also exhibit respiratory and feeding difficulties. Cases of Pierre Robin Sequence are both phenotypically and genetically heterogeneous (Cohen, 1999; Houdayer et al., 2001; Jakobsen et al., 2006; Jamshidi et al., 2004; Melkoniemi et al., 2003; Ounap et al., 2005; Ricks et al., 2002). Pierre Robin Sequence can occur as an isolated nonsyndromic form, or can occur in combination with other syndromes. Mutations in several collagen genes, including *COL2A1*, *COL11A1* and *COL11A2*, have been found in subjects with nonsyndromic Pierre Robin Sequence (Melkoniemi et al., 2003), although it has not been established definitively that these mutations are causal for the observed malformations. In addition, chromosomal translocations (Jamshidi et al., 2004), duplications (Ounap et al., 2005) and deletions (Houdayer et al., 2001) have been described that are associated with nonsyndromic Pierre Robin Sequence.

A model for the etiology of the cleft palate defect in individuals with Pierre Robin Sequence is that the small and/or abnormally positioned mandible prevents the normal positioning of the tongue, thereby inhibiting palatal shelf elevation and fusion. This model is supported by analyses of two mouse models of Pierre Robin Sequence, the A/WySn inbred mouse strain (Schubert et al., 2005) and mice heterozygous for the disproportionate micromelia (*Dmm*) mutation (Ricks et al., 2002), a semidominant mutant allele of the *Col2a1* gene (Pace et al., 1997). Based on a mechanical requirement for mandibular extension to drive the proper depression of the tongue, we propose that a similar mechanism is responsible for the cleft palate phenotype of *Snai1/2-dko* mice. This interpretation is supported by the dramatic growth retardation of Meckel's cartilage at E14.5, the crucial time for palatal shelf elevation. *Snai1/2-dko* mice represent a novel model of Pierre Robin Sequence, and should provide a useful tool for the study of this heterogeneous developmental disorder in humans.

We thank Rulang Jiang for providing probes, and members of the Gridley lab for comments and suggestions. This work was supported by a grant from the American Cancer Society to S.A.M. (PF-04-245-01-DDC) and grants from the NIH to T.G. (HD034883) and the Jackson Laboratory (CA034196).

Supplementary material

Supplementary material for this article is available at http://dev.biologists.org/cgi/content/full/134/9/1789/DC1

References

Barrallo-Gimeno, A. and Nieto, M. A. (2005). The Snail genes as inducers of cell movement and survival: implications in development and cancer. *Development* **132**, 3151-3161.

Batlle, E., Sancho, E., Franci, C., Dominguez, D., Monfar, M., Baulida, J. and Garcia De Herreros, A. (2000). The transcription factor snail is a repressor of E-cadherin gene expression in epithelial tumour cells. *Nat. Cell Biol.* **2**, 84-89.

Brewer, S., Feng, W., Huang, J., Sullivan, S. and Williams, T. (2004). Wnt1-Cre-mediated deletion of AP-2alpha causes multiple neural crest-related defects. *Dev. Biol.* **267**, 135-152.

Cano, A., Perez-Moreno, M. A., Rodrigo, I., Locascio, A., Blanco, M. J., del Barrio, M. G., Portillo, F. and Nieto, M. A. (2000). The transcription factor snail controls epithelial-mesenchymal transitions by repressing E-cadherin expression. *Nat. Cell Biol.* **2**, 76-83.

Carette, M. J. and Ferguson, M. W. (1992). The fate of medial edge epithelial cells during palatal fusion in vitro: an analysis by DiI labelling and confocal microscopy. *Development* **114**, 379-388.

Carver, E. A., Jiang, R., Lan, Y., Oram, K. F. and Gridley, T. (2001). The mouse snail gene encodes a key regulator of the epithelial-mesenchymal transition. *Mol. Cell. Biol.* **21**, 8184-8188.

Casey, L. M., Lan, Y., Cho, E. S., Maltby, K. M., Gridley, T. and Jiang, R. (2006). Jag2-Notch1 signaling regulates oral epithelial differentiation and palate development. *Dev. Dyn.* **235**, 1830-1844.
Cohen, M. M., Jr (1999). Robin sequences and complexes: causal heterogeneity and pathogenetic/phenotypic variability. *Am. J. Med. Genet.* **84**, 311-315.
Cuervo, R. and Covarrubias, L. (2004). Death is the major fate of medial edge epithelial cells and the cause of basal lamina degradation during palatogenesis. *Development* **131**, 15-24.
Cuervo, R., Valencia, C., Chandraratna, R. A. and Covarrubias, L. (2002). Programmed cell death is required for palate shelf fusion and is regulated by retinoic acid. *Dev. Biol.* **245**, 145-156.
Danielian, P. S., Muccino, D., Rowitch, D. H., Michael, S. K. and McMahon, A. P. (1998). Modification of gene activity in mouse embryos in utero by a tamoxifen-inducible form of Cre recombinase. *Curr. Biol.* **8**, 1323-1326.
Dudas, M., Sridurongrit, S., Nagy, A., Okazaki, K. and Kaartinen, V. (2004). Craniofacial defects in mice lacking BMP type I receptor Alk2 in neural crest cells. *Mech. Dev.* **121**, 173-182.
Ferguson, M. W. (1988). Palate development. *Development* **103**, S41-S60.
Fitchett, J. E. and Hay, E. D. (1989). Medial edge epithelium transforms to mesenchyme after embryonic palatal shelves fuse. *Dev. Biol.* **131**, 455-474.
Gato, A., Martinez, M. L., Tudela, C., Alonso, I., Moro, J. A., Formoso, M. A., Ferguson, M. W. and Martinez-Alvarez, C. (2002). TGF-beta(3)-induced chondroitin sulphate proteoglycan mediates palatal shelf adhesion. *Dev. Biol.* **250**, 393-405.
Gendron-Maguire, M., Mallo, M., Zhang, M. and Gridley, T. (1993). Hoxa-2 mutant mice exhibit homeotic transformation of skeletal elements derived from cranial neural crest. *Cell* **75**, 1317-1331.
Gorlin, R. J., Cohen, M. M. and Hennekam, R. C. M. (2001). *Syndromes of the Head and Neck*. Oxford, New York: Oxford University Press.
Houdayer, C., Portnoi, M. F., Vialard, F., Soupre, V., Crumiere, C., Taillemite, J. L., Couderc, R., Vazquez, M. P. and Bahuau, M. (2001). Pierre Robin sequence and interstitial deletion 2q32.3-q33.2. *Am. J. Med. Genet.* **102**, 219-226.
Ingham, P. W. and McMahon, A. P. (2001). Hedgehog signaling in animal development: paradigms and principles. *Genes Dev.* **15**, 3059-3087.
Inoue, A., Seidel, M. G., Wu, W., Kamizono, S., Ferrando, A. A., Bronson, R. T., Iwasaki, H., Akashi, K., Morimoto, A., Hitzler, J. K. et al. (2002). Slug, a highly conserved zinc finger transcriptional repressor, protects hematopoietic progenitor cells from radiation-induced apoptosis in vivo. *Cancer Cell* **2**, 279-288.
Inukai, T., Inoue, A., Kurosawa, H., Goi, K., Shinjyo, T., Ozawa, K., Mao, M., Inaba, T. and Look, A. T. (1999). SLUG, a ces-1-related zinc finger transcription factor gene with antiapoptotic activity, is a downstream target of the E2A-HLF oncoprotein. *Mol. Cell* **4**, 343-352.
Ito, Y., Yeo, J. Y., Chytil, A., Han, J., Bringas, P., Jr, Nakajima, A., Shuler, C. F., Moses, H. L. and Chai, Y. (2003). Conditional inactivation of Tgfbr2 in cranial neural crest causes cleft palate and calvaria defects. *Development* **130**, 5269-5280.
Jakobsen, L. P., Knudsen, M. A., Lespinasse, J., Garcia Ayuso, C., Ramos, C., Fryns, J. P., Bugge, M. and Tommerup, N. (2006). The genetic basis of the Pierre Robin Sequence. *Cleft Palate Craniofac. J.* **43**, 155-159.
Jamshidi, N., Macciocca, I., Dargaville, P. A., Thomas, P., Kilpatrick, N., McKinlay Gardner, R. J. and Farlie, P. G. (2004). Isolated Robin sequence associated with a balanced t(2;17) chromosomal translocation. *J. Med. Genet.* **41**, e1.
Jiang, R., Lan, Y., Chapman, H. D., Shawber, C., Norton, C. R., Serreze, D. V., Weinmaster, G. and Gridley, T. (1998a). Defects in limb, craniofacial, and thymic development in Jagged2 mutant mice. *Genes Dev.* **12**, 1046-1057.
Jiang, R., Lan, Y., Norton, C. R., Sundberg, J. P. and Gridley, T. (1998b). The Slug gene is not essential for mesoderm or neural crest development in mice. *Dev. Biol.* **198**, 277-285.
Kaartinen, V., Voncken, J. W., Shuler, C., Warburton, D., Bu, D., Heisterkamp, N. and Groffen, J. (1995). Abnormal lung development and cleft palate in mice lacking TGF-beta 3 indicates defects of epithelial-mesenchymal interaction. *Nat. Genet.* **11**, 415-421.
Knight, A. S., Schutte, B. C., Jiang, R. and Dixon, M. J. (2006). Developmental expression analysis of the mouse and chick orthologues of IRF6: the gene mutated in Van der Woude syndrome. *Dev. Dyn.* **235**, 1441-1447.
Kondo, S., Schutte, B. C., Richardson, R. J., Bjork, B. C., Knight, A. S., Watanabe, Y., Howard, E., de Lima, R. L., Daack-Hirsch, S., Sander, A. et al. (2002). Mutations in IRF6 cause Van der Woude and popliteal pterygium syndromes. *Nat. Genet.* **32**, 285-289.
Krebs, L. T., Deftos, M. L., Bevan, M. J. and Gridley, T. (2001). The Nrarp gene encodes an ankyrin-repeat protein that is transcriptionally regulated by the notch signaling pathway. *Dev. Biol.* **238**, 110-119.
Lan, Y., Ovitt, C. E., Cho, E. S., Maltby, K. M., Wang, Q. and Jiang, R. (2004). Odd-skipped related 2 (Osr2) encodes a key intrinsic regulator of secondary palate growth and morphogenesis. *Development* **131**, 3207-3216.
Lidral, A. C., Romitti, P. A., Basart, A. M., Doetschman, T., Leysens, N. J., Daack-Hirsch, S., Semina, E. V., Johnson, L. R., Machida, J., Burds, A. et al. (1998). Association of MSX1 and TGFB3 with nonsyndromic clefting in humans. *Am. J. Hum. Genet.* **63**, 557-568.
Locascio, A., Manzanares, M., Blanco, M. J. and Nieto, M. A. (2002). Modularity and reshuffling of Snail and Slug expression during vertebrate evolution. *Proc. Natl. Acad. Sci. USA* **99**, 16841-16846.
Mao, X., Fujiwara, Y., Chapdelaine, A., Yang, H. and Orkin, S. H. (2001). Activation of EGFP expression by Cre-mediated excision in a new ROSA26 reporter mouse strain. *Blood* **97**, 324-326.
Martinez-Alvarez, C., Bonelli, R., Tudela, C., Gato, A., Mena, J., O'Kane, S. and Ferguson, M. W. (2000a). Bulging medial edge epithelial cells and palatal fusion. *Int. J. Dev. Biol.* **44**, 331-335.
Martinez-Alvarez, C., Tudela, C., Perez-Miguelsanz, J., O'Kane, S., Puerta, J. and Ferguson, M. W. (2000b). Medial edge epithelial cell fate during palatal fusion. *Dev. Biol.* **220**, 343-357.
Martinez-Alvarez, C., Blanco, M. J., Perez, R., Rabadan, M. A., Aparicio, M., Resel, E., Martinez, T. and Nieto, M. A. (2004). Snail family members and cell survival in physiological and pathological cleft palates. *Dev. Biol.* **265**, 207-218.
Mazzalupo, S. and Coulombe, P. A. (2001). A reporter transgene based on a human keratin 6 gene promoter is specifically expressed in the periderm of mouse embryos. *Mech. Dev.* **100**, 65-69.
Melkoniemi, M., Koillinen, H., Mannikko, M., Warman, M. L., Pihlajamaa, T., Kaariainen, H., Rautio, J., Hukki, J., Stofko, J. A., Cisneros, G. J. et al. (2003). Collagen XI sequence variations in nonsyndromic cleft palate, Robin sequence and micrognathia. *Eur. J. Hum. Genet.* **11**, 265-270.
Miettinen, P. J., Chin, J. R., Shum, L., Slavkin, H. C., Shuler, C. F., Derynck, R. and Werb, Z. (1999). Epidermal growth factor receptor function is necessary for normal craniofacial development and palate closure. *Nat. Genet.* **22**, 69-73.
Murray, J. C. (2002). Gene/environment causes of cleft lip and/or palate. *Clin. Genet.* **61**, 248-256.
Murray, S. A. and Gridley, T. (2006). Snail family genes are required for left-right asymmetry determination, but not neural crest formation, in mice. *Proc. Natl. Acad. Sci. USA* **103**, 10300-10304.
Murray, S. A., Carver, E. A. and Gridley, T. (2006). Generation of a Snail1 (Snai1) conditional null allele. *Genesis* **44**, 7-11.
Nawshad, A., LaGamba, D. and Hay, E. D. (2004). Transforming growth factor beta (TGFbeta) signalling in palatal growth, apoptosis and epithelial mesenchymal transformation (EMT). *Arch. Oral Biol.* **49**, 675-689.
Nieto, M. A. (2002). The snail superfamily of zinc-finger transcription factors. *Nat. Rev. Mol. Cell Biol.* **3**, 155-166.
Nieto, M. A., Sargent, M. G., Wilkinson, D. G. and Cooke, J. (1994). Control of cell behavior during vertebrate development by Slug, a zinc finger gene. *Science* **264**, 835-839.
Oram, K. F. and Gridley, T. (2005). Mutations in snail family genes enhance craniosynostosis of Twist1 haplo-insufficient mice: implications for Saethre-Chotzen Syndrome. *Genetics* **170**, 971-974.
Oram, K. F., Carver, E. A. and Gridley, T. (2003). Slug expression during organogenesis in mice. *Anat. Rec. A Discov. Mol. Cell. Evol. Biol.* **271**, 189-191.
Ounap, K., Ilus, T., Laidre, P., Uibo, O., Tammur, P. and Bartsch, O. (2005). A new case of 2q duplication supports either a locus for orofacial clefting between markers D2S1897 and D2S2023 or a locus for cleft palate only on chromosome 2q13-q21. *Am. J. Med. Genet. A* **137**, 323-327.
Pace, J. M., Li, Y., Seegmiller, R. E., Teuscher, C., Taylor, B. A. and Olsen, B. R. (1997). Disproportionate micromelia (Dmm) in mice caused by a mutation in the C-propeptide coding region of Col2a1. *Dev. Dyn.* **208**, 25-33.
Peters, H., Neubuser, A., Kratochwil, K. and Balling, R. (1998). Pax9-deficient mice lack pharyngeal pouch derivatives and teeth and exhibit craniofacial and limb abnormalities. *Genes Dev.* **12**, 2735-2747.
Rice, R., Spencer-Dene, B., Connor, E. C., Gritli-Linde, A., McMahon, A. P., Dickson, C., Thesleff, I. and Rice, D. P. (2004). Disruption of Fgf10/Fgfr2b-coordinated epithelial-mesenchymal interactions causes cleft palate. *J. Clin. Invest.* **113**, 1692-1700.
Ricks, J. E., Ryder, V. M., Bridgewater, L. C., Schaalje, B. and Seegmiller, R. E. (2002). Altered mandibular development precedes the time of palate closure in mice homozygous for disproportionate micromelia: an oral clefting model supporting the Pierre-Robin sequence. *Teratology* **65**, 116-120.
Schubert, J., Jahn, H. and Berginski, M. (2005). Experimental aspects of the pathogenesis of Robin sequence. *Cleft Palate Craniofac. J.* **42**, 372-376.
Sefton, M., Sanchez, S. and Nieto, M. A. (1998). Conserved and divergent roles for members of the Snail family of transcription factors in the chick and mouse embryo. *Development* **125**, 3111-3121.
Taya, Y., O'Kane, S. and Ferguson, M. W. (1999). Pathogenesis of cleft palate in TGF-beta3 knockout mice. *Development* **126**, 3869-3879.
Tudela, C., Formoso, M. A., Martinez, T., Perez, R., Aparicio, M., Maestro, C., Del Rio, A., Martinez, E., Ferguson, M. and Martinez-Alvarez, C. (2002). TGF-beta3 is required for the adhesion and intercalation of medial edge epithelial cells during palate fusion. *Int. J. Dev. Biol.* **46**, 333-336.